Articles

The Equilibrium Folding Pathway of Staphylococcal Nuclease: Identification of the Most Stable Chain−Chain Interactions by NMR and CD Spectroscopy†

Yi Wang and David Shortle*

Department of Biological Chemistry, The Johns Hopkins University School of Medicine, Baltimore, Maryland 21205

Received July 28, 1995; Revised Manuscript Received September 21, 1995®

ABSTRACT: In a previous report [Alexandrescu, A. T., Abeygunawardana, C., & Shortle, D. (1994) *Biochemistry 33*, 1063−1072], NMR methods were used to characterize the residual structure in Δ131Δ, a large fragment of staphylococcal nuclease that serves as a model denatured state under nondenaturing conditions. On the basis of a large number of missing amide protons for the residues that form a three-strand antiparallel β sheet in the native state, it was concluded that this β meander may be highly populated in Δ131Δ, with severe line broadening due to relatively slow exchange between different conformational states. In the present report, results from circular dichroism spectroscopy and NMR spectroscopy indicate strands β2-β3 form a β hairpin at urea concentrations below 6 M. Amide proton resonances from several hydrophobic residues adjacent to this β hairpin disappear in concert with all of the β2-β3 residues, suggesting a local, non-native hydrophobic interaction may help stabilize the beta hairpin. At concentrations below 3 M, all amide resonances from strand β1 in Δ131Δ also disappear, suggesting that β1 may combine with the β2-β3 hairpin to form a native-like β meander. In addition, the hydrophobic helix α2 decreases from approximately 30% population in 0 M urea to approximately 10%−15% at 6 M urea, whereas helix α1 goes from 10%−15% populated in 0 M urea to undetectable in 6 M urea. Characterization of a second, distinctly different denatured state, WT nuclease at pH 3.0 and low salt, reveals that this low-density acid-denatured state is structurally similar to Δ131Δ at low concentrations of urea. From these and previously published data, a tenative equilibrium folding pathway can be constructed for staphylococcal nuclease which describes the relative strengths and interdependencies of the chain−chain interactions involved in forming the native state.

In the past few years, it has become clear that not all chain−chain interactions are lost when the native state of a protein undergo reversible denaturation (Kuwajima, 1989; Dill & Shortle, 1991; Dobson, 1992; Shortle, 1993). In the small number of cases in which structural information has been obtained, this persistent, residual structure involves hydrophobic interactions between residues in close proximity along the chain (Neri et al., 1992; Logan et al., 1994; Alexandrescu et al., 1994a). Such residual structure must play a significant role in the energetics of protein folding. On the one hand, if these structures are native-like, then they represent early folding elements which can be retained during subsequent steps as the polypeptide chain advances toward the native state. On the other hand, if these residual structures are not native-like, they must be undone at some cost in free energy before folding can continue. In other words, residual structure that does not contribute to the final folded state serves to slow the process of folding and destabilize the native state indirectly by lowering the free energy of the denatured state.

Many small, single-domain proteins fold very rapidly, often within a few milliseconds after transfer from denaturing to native conditions (Matthews, 1993). Perhaps the simplest explanation for this remarkable feature is that many, perhaps most, of the chain−chain interactions that persist in the denatured state are retained in part or in full in later folding intermediates. Thus early folding steps would involve local interactions within several relatively independent chain segments. Later steps in folding then involve the merger or fusion of local structures in a hierarchical manner, leading to the orderly buildup of the native state through intermediates of increasing native-like character.

One experimental strategy for defining this buildup of structure is to characterize the persistent structure in the denatured state of a protein in a sequence of equilibrium steps in which the conditions of solution are changed (Shortle, 1993; Wang et al., 1995). By varying the urea concentration, the temperature, or the pH, it should be possible to vary the "free energy distance" between a polypeptide chain frustrated in its attempts to fold and the native state, the end point of folding. By definition, the most stable interactions are those which persist under the most unfavorable conditions, such as high urea concentration or high temperature. As conditions are made more favorable for folding (e.g., high glycerol concentrations), weaker chain−chain interactions can form, building upon more stable structures. In this way an equilibrium folding pathway can be experimentally defined, a pathway which may not reflect

† This research is supported by a grant from the NIH to D.S. (GM-34171).

* To whom correspondence should be addressed.

® Abstract published in *Advance ACS Abstracts,* November 15, 1995.

0006-2960/95/0434-15895$09.00/0

the sequence of kinetic events during real-time folding but instead gives insight into the energetics of the structure assembly process.

NMR spectroscopy is well suited for characterization of partially folded states of proteins. Information about dihedral angles or proximity to other residues can potentially be obtained for specific residues within the polypeptide chain. Although most NMR parameters will be time-averaged over the ensemble of structures present, such averaging can be viewed as a filter that allows identification of the properties of only the most highly populated conformations. Early work on denatured proteins has revealed some of the difficulties and potential limitations of NMR spectroscopy to extract information about partially folded proteins (Logan et al., 1994; Shortle & Abeygunawardana, 1993; Alexandrescu et al., 1994), making it clear that the structure of partially folded proteins cannot be described in anything like the detail of the native state. Nevertheless, NMR characterization of non-native states of proteins is an area of investigation still in its infancy, and new NMR experiments plus improvements in NMR instrumentation can be expected to provide information sufficient to define many of the general features of denatured-state structure and dynamic behavior.

Staphylococcal nuclease is an attractive system for studying both the energetics of folding and the residual structure in partially folded forms. A small protein of 149 residues with no prosthetic groups or cysteines, staphylococcal nuclease is highly soluble in both the native and denatured states. A large fragment, designated Δ131Δ, has been developed as a model denatured state under physiological conditions (Alexandrescu et al., 1994; Alexandrescu & Shortle, 1994). Lacking only six residues from the amino terminus and one residue from the carboxy terminus that occupy fixed positions in the native state, Δ131Δ is at least 99.5% denatured at pH 7.0 and 20 °C. Yet, upon addition of substrate or the active site ligands calcium ion and 3′,5′-thymidine diphosphate, Δ131Δ refolds to a state that is virtually identical to native nuclease.

Sequential assignment of the backbone resonances of Δ131Δ at pH 5.3 and 32 °C has defined several residual secondary structures. Shown diagrammatically in Figure 1, these include (1) 30% population of α helix 2 (α2), (2) 10%−20% population of helix α1, and (3) significant population of two native-like turns, a Type I turn involving residues 83−87 and a Type I′ turn (residues 94−97). Although no evidence for β strand formation was detected for strands β4 and β5, it was noted that almost all of the amide protons for the chain segment corresponding to β1, β2, and β3 were missing from the $^{15}N-^{1}H$ correlation spectrum. In view of the fact that conformational exchange between different structures with different chemical shifts is the only known mechanism that could lead to such severe broadening of a contiguous stretch of resonances under the conditions of these experiments, it was proposed that the three-strand antiparallel sheet is probably significantly populated in Δ131Δ (Alexandrescu et al., 1994).

In this report, we describe an analysis of the effects of urea and low pH on the residual structure in this model denatured state of staphylococcal nuclease. Circular dichroism and NMR spectroscopy are used to characterize the structural changes produced as the "free energy distance" between denatured and native nuclease is increased by these two denaturants. In addition to permitting the identification of the most stable chain−chain interactions, these data confirm that most but not all of the residual structure observed in the large fragment Δ131Δ is also present in a distinctly different denatured state, namely full-length wild-type (WT) nuclease denatured by low pH at low salt concentrations.

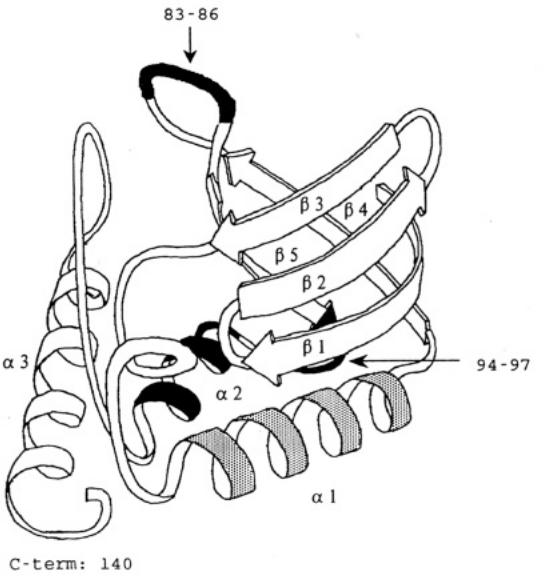

FIGURE 1: Ribbon diagram of native staphylococcal nuclease representing the segments of native-like residual structure previously identified in Δ131Δ (black, most persistent; gray, less persistent). Δ131Δ consists of residues 1−3 and 13−140 (i.e., residues 4−12 and 141−149 have been deleted). The three helices (α1, 54−67; α2, 98−106; α3, 121−135), five β strands (β1, 13−19; β2, 21−27; β3, 29−35; β4, 71−76; β5, 90−95), and two reverse turns (83−86 and 94−97) are labeled. Modified from Alexandrescu et al. (1994).

EXPERIMENTAL PROCEDURES

Samples for Δ131Δ and WT full-length nuclease uniformly enriched for ^{15}N or for ^{15}N and ^{13}C were prepared according to previously published methods (Alexandrescu et al., 1994). After extensive dialysis against distilled H_2O and lyophilization, preparations of Δ131Δ in 10% D_2O and 1 mM sodium azide were adjusted to pH 5.3 with 1 N HCl. Solid urea was added to a final concentration of 6 M without further adjustment of the pH. Similarly, after dialysis against distilled H_2O, samples of WT nuclease in 10% D_2O and 1 mM sodium azide were titrated to a final pH of 3.0 using 1 N HCl. To obtain $\{^{1}H,^{15}N\}$-HSQC spectra at urea concentrations from 1 to 7 M, 1.5 mM solutions of Δ131Δ at pH 5.3 in 8% D_2O were made up at 0 and at 8 M urea and then were mixed in the appropriate ratios to give the final urea concentration at constant protein concentration.

Circular dichroism spectra were collected on an AVIV DS60 spectrometer in a 0.1 mm path length cuvette thermostated at 32 °C. Urea titrations were carried out in 20 mM acetate buffer (pH 5.3) or 20 mM glycine buffer (pH 3.0) on protein samples with a final concentration of 1.2 mg/mL. For each spectrum, five scans collected at 0.5 nm increments were added, smoothed and then corrected for the contribution of buffer and cell.

All NMR spectra were collected on a Varian Unity Plus 600 MHz spectrometer at 32 °C using concentrations of protein between 1.5 and 3.0 mM. $\{^{1}H,^{15}N\}$-HSQC spectra

were obtained by using the pulse sequence of Mori et al. (1995) with the carrier frequency set on the water peak (4.71 ppm), typically with 512 complex points in t_2 (sw = 6000 Hz) and 128 complex points in t_1 (sw = 1300 Hz). $^{15}N-^{1}H$ correlation spectra were also obtained by cross-polarization using a 9 ms DIPSI-2-based spin lock on both ^{1}H and ^{15}N (3165 Hz field) in forward and reverse directions. The ^{1}H carrier frequency was set at 8.1 ppm, and the ^{15}N carrier frequency was set at 120 ppm. To obtain an HSQC spectrum with the same 9 ms transfer time instead of the typical 4.5 ms, a ^{1}H spin echo of total duration 4.5 ms was added to the conventional HSQC pulse sequence immediately before and immediately after t_1. In addition, an $\{^{1}H,^{15}N\}$-HSQC with double-refocused INEPT was carried with a 9 ms transfer time using the method of Morris and Freeman (1979). For all 2D experiments, the data size of each dimension was doubled by zero filling.

The HNCACB spectra were obtained using the sensitivity-enhanced pulse sequence of Muhandiram and Kay (1994), with 512 complex points in t_3 (^{1}H, sw = 6000 Hz), 64 complex points in t_1 (^{13}C, sw = 8300 Hz), and 32 complex points in t_2 (^{15}N, sw = 1400 Hz). Similarly, the HNCO spectrum (Muhandiram & Kay, 1994) consisted of 512 complex points in t_3 (^{1}H, sw = 6000 Hz), 96 complex points in t_1 (^{13}C, sw = 905 Hz, carrier frequency = 176.16 ppm), and 32 complex points in t_2 (^{15}N, sw = 1400 Hz). For both the HNCACB and the HNCO experiments, each dimension was doubled in size by zero filling. The $\{^{1}H,^{15}N\}$-TOCSY-HSQC spectra (Kay et al., 1992) employed a 8.9 kHz field for 53 ms of isotropic mixing using DIPSI-2. Spectral widths were 6000, 1160, and 6000 Hz in t_1 (^{1}H), t_2 (^{15}N), and t_3 (^{1}H), respectively; 84, 40, and 512 complexes points were collected, respectively, with zero filling to final data files of 256, 128, and 1024 points. The $\{^{1}H-^{15}N\}$-NOESY-HSQC spectra (Kay et al., 1992) was collected with a 200 ms mixing time using the same spectral widths and data sizes as for the $\{^{1}H-^{15}N\}$-TOCSY-HSQC. Data were processed using FELIX 1.1, peaks were selected manually, and data were stored and manipulated using the spreadsheet program EXCEL. In all experiments, several levels of resolution enhancement were applied to the directly detected ^{1}H dimension, with most analysis being done on spectra apodized with a sine bell shifted by 15°. A sine bell shifted between 45 and 90° was used for apodization of all indirectly detected dimensions.

RESULTS

Δ131Δ in Urea. As shown in Figure 2A, the far-ultraviolet CD[1] spectrum of Δ131Δ reveals a shallow minimum between 210 and 230 nm, consistent with a small amount of residual secondary structure. As urea is added to Δ131Δ, the minimum between 210 and 230 becomes less pronounced, and by 6 M urea has been almost entirely eliminated. The difference between spectra at 2, 4 and 6 M urea versus the spectrum at 0 M urea approximates the CD spectrum of the structure that has been lost on addition of urea to that final concentration. As shown in Figure 2B, each of these three difference spectra exhibits a single

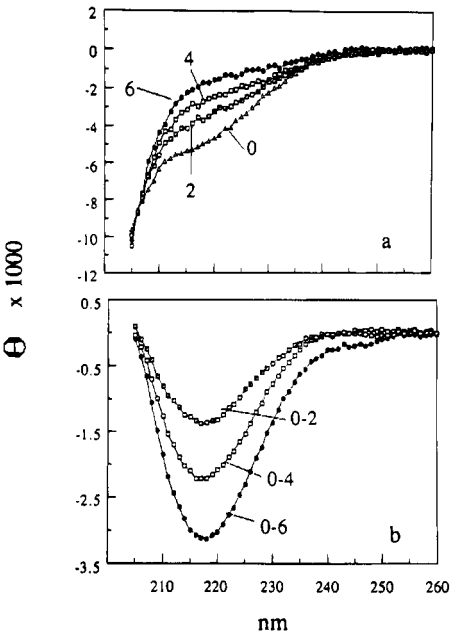

FIGURE 2: (A) Far-ultraviolet circular dichroism spectra of Δ131Δ as a function of urea concentration: 0, 2, 4, and 6 M. The *y*-axis is the ellipticity in deg cm^2 dmol^{-1}. (B) Difference spectra obtained by subtracting the 2, 4, and 6 M spectra from the 0 M urea spectrum, to approximate the spectra of the structure lost upon addition of urea.

minimum near 215 nm characteristic of β sheet structure (Johnson, 1988). Difference spectra obtained without and with guanidine hydrochloride gave this same minimum near 215 nm, with the CD spectrum in 2.5 M GuHCl being equivalent to that in 6 M urea (data not shown).[2]

While previous NMR analyses of Δ131Δ have not yielded unequivocal evidence of any β structure, it is noteworthy that all of the amide proton peaks for residues 13−42 are missing from the $^{15}N-^{1}H$ correlation spectrum (Alexandrescu et al., 1994). (Initial assignments of peaks to K24, L25, M26, Y27, G29, M32, T33, and V39 appear to have been in error, in many cases caused by minor peaks due to nearby proline isomers.) In view of the relatively low pH used and the sharp lines observed with many protons known to be highly solvent exposed, the only plausible mechanism for the severe broadening of these H_N resonances is exchange between two or more conformations, either between a structured conformation and an unstructured conformation or between two or more structured conformations. If these different conformations display large differences in ^{1}H and/or ^{15}N chemical shifts, then exchange rates on the order of 0.1−1.0 per millisecond would lead to severe line broadening (Abragam, 1961; Jardetsky & Roberts, 1981).

The effect of urea on the ^{15}N-^{1}H correlation spectrum of Δ131Δ was determined to test the hypothesis that one of

[1] Abbreviations: CD, circular dichroism; GuHCl, guanidine hydrochloride; NMR, nuclear magnetic resonance; HSQC, heteronuclear single-quantum coherence; NOESY, nuclear Overhauser effect spectroscopy; TOCSY, total correlation spectroscopy, WT, wild-type.

[2] Although urea has been reported to induce a peak of positive ellipticity at 217 nm for some homopolypeptides [reviewed in Woody (1992)], in these same cases GuHCl at concentrations below 2.5 M has had the opposite effect. The similarity between the spectra of Δ131Δ in 6 M urea and in 2.5 M GuHCl plus the absence of any changes in the CD spectrum of trypsin-digested Δ131Δ (which completely removes the shallow CD minimum between 210 and 230 (Shortle & Meeker, 1989) in 0 versus 6 M urea (data not shown) strongly suggest that the observed changes in the circular dichroism spectra of Δ131Δ in urea reflect loss of a preexisting β structure, not the artifactual induction of new secondary structure such as the polyproline helix (Tiffany & Krimm, 1973).

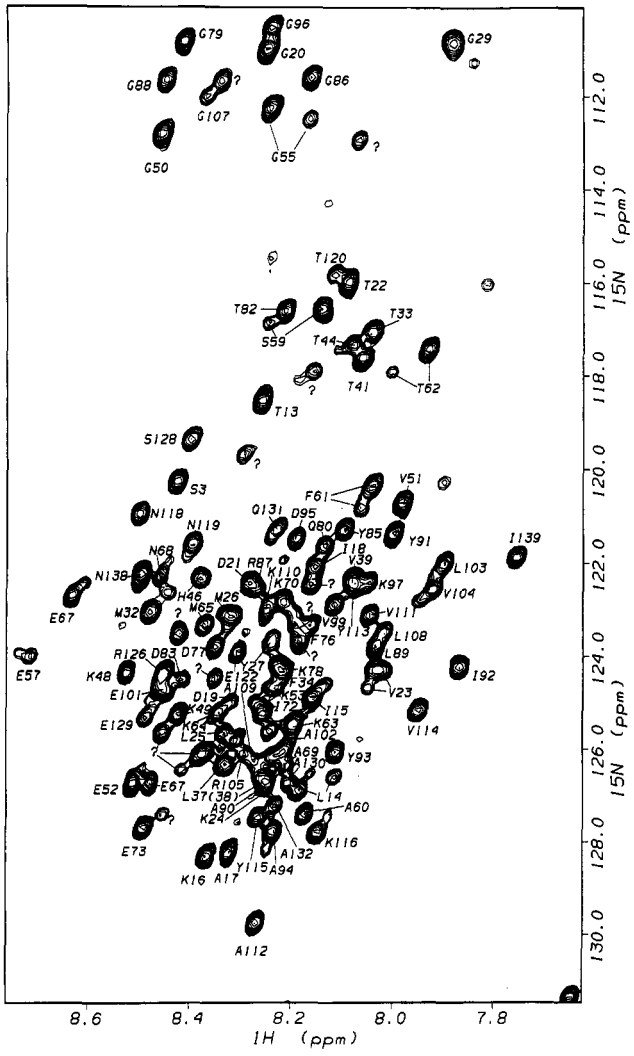

FIGURE 3: $^{15}N-^{1}H$ correlation spectrum (HSQC) of Δ131Δ in 6 M urea at pH 5.3, 32 °C, with peak assignments.

these conformations is highly ordered, such as the β1-β2-β3 meander formed by these residues in the native state. At some concentration of urea, most ordered conformations break down as hydrophobic interactions are weakened, which should lead to the appearance of amide proton peaks from the more averaged, random coil-like state. Between 0 and 3 M urea, no new peaks were observed, and all H_N resonances except three (I92, Y93, and G107) showed minimal or no detectable changes in either ^{15}N or ^{1}H chemical shifts. However, at 4 M urea six new peaks were clearly resolved, six more newly resolved peaks appeared at 5 M urea, and 11 more appeared at 6 M urea. (The assigned spectrum in 6 M urea is shown in Figure 3.) No additional peaks could be identified in 7 M urea. Most of the new peaks continued to grow in intensity with increasing urea concentrations. These findings strongly support the existence of a transition between a structured and a random coil-like state.

NMR characterization of any structure builds upon observable resonances. Since none of the H_N protons of the β1-β2-β3 segment can be detected in the absence of urea, an attempt was made to identify the H_α resonances of some of these residues (phenylalanine F34; leucines L14, L25, L36, L37, and L38; and isoleucines I15 and I18) using specific labeling with uniform ^{13}C amino acids. In the ^{13}C-selected 1D proton spectrum, only the previously assigned resonances

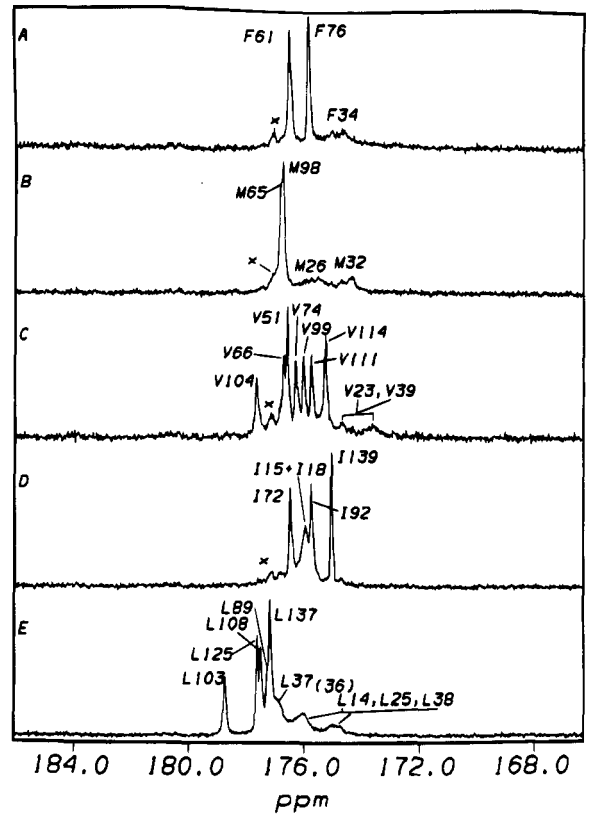

FIGURE 4: The directly detected ^{13}C carbonyl spectra of Δ131Δ labeled with a single amino acid containing ^{13}C at the carbonyl position only. Data were collected at 150.8 MHz using a broad band probe by adding 2048 transients of 608 complex points. The carrier frequency was set at 176.16 ppm, with a spectral width of 3000 Hz. Before Fourier transformation, the FID was multiplied by an exponential function which broadened the lines by 8 Hz and zero filled to 1024 points. A, phenylalanine; B, methionine; C, valine; D, isoleucine; E, leucine.

for residues outside the β1-β2-β3 segment could be identified with certainty. In a two-dimensional $^{1}H-^{13}C(O)$ correlation experiment, the H_α of F34 was observed as a very weak peak at 4.66 ppm. Similar experiments with labeled leucine and isoleucine detected several extremely weak peaks in addition to the expected strong signals from the leucines/isoleucines outside of the β1-β2-β3 segment. These results suggest that either the H_α and/or the $^{13}C_\alpha/^{13}C(O)$ resonances also experience severe line broadening.

Since the ^{13}C resonance of the backbone carbonyl carbon $^{13}C(O)$ is often the sharpest line in large proteins, attempts were made to directly detect this signal from the "missing residues" in β1-β2-β3 by labeling Δ131Δ with single amino acids (phenylalanine, methionine, isoleucine, leucine, and valine) with ^{13}C incorporated at the carbonyl position only. These spectra, shown in Figure 4, reveal broad, upfield-shifted peaks for nearly all of the residues in question. The fact that all of these peaks in 0 M urea are shifted upfield relative to both their values in 6 M urea (obtained from the HNCO experiment) strongly supports that the conclusion that this chain segment is in a β sheet conformation (Wishart et al., 1991).

Using the known chemical shifts of the assigned ^{13}C carbonyls F61 and F76 (Alexandrescu et al., 1994), F34 could be assigned to the weak upfield peak. To resolve the ambiguity among the possible assignments for the other new peaks, ^{13}C spectra were obtained in urea at 1 M increments

from 0 to 7 M urea. With increasing urea, the broad, upfield peaks either sharpened and shifted smoothly downfield (I15, I18, M26) or diminished in intensity followed by the appearance of downfield peaks which then sharpened (F34, M32, V23, V39). To assign all carbonyls in 6 M urea, a three-dimensional HNCO experiment was carried out with uniformly $^{15}N-^{13}C$ labeled Δ131Δ. With these assignments, the carbonyl peaks in the absence of urea could be assigned to one or a small number of possible residues (Figure 4) by tracking all peaks from 6 to 0 M urea.

The severe broadening of the H_N and the $^{13}C(O)$ resonances of the β1-β2-β3 segment, and presumably H_α, ^{15}N, and $^{13}C_\alpha$ resonances as well, could result from either of two dynamic mechanisms occurring in the 1−10 millisecond time range: (1) exchange between a structured conformation and a random coil-like state or (2) intermediate exchange between multiple alternate stuctured conformations, such as warping or twisting of the β sheet, with slow exchange with the random coil-like state.

To attempt to distinguish between these two possibilites, $^{15}N-^{1}H$ correlation spectra of Δ131Δ at 3.5 M urea were obtained using three pulse sequences with different sensitivities to line broadening due to conformational exchange. A spectrum obtained by cross-polarization should experience no relaxation by this T_2 mechanism during the delays required for magnetization transfer from protons to nitrogen and back (Yamazaki et al., 1995), since a spin lock on both ^{1}H and ^{15}N is employed to affect this transfer. However, in a conventional HSQC experiment, relaxation caused by conformational exchange will occur during magnetization transfer, leading to a peak with reduced intensity. Since all other contributions to T_2 relaxation for H_N and ^{15}N are the same for the two types of experiment, a comparison of the relative peaks heights should provide a qualitative measure of the amount of broadening caused by exchange between the random coil-like state and the structured state.

As can be seen in Figure 5, the intensity of two peaks from the β1 segment (K16 and A17) varies slightly as the time allowed for ^{1}H chemical shift evolution is varied during the magnetization transfer steps from ^{1}H to ^{15}N and back. When this time is decreased from a total of 18 ms (panel A) to 9 ms (panel B) to 0 ms (panel C), the intensity of these two peaks increases by approximately 30%. This result suggests that only a relatively small fraction of the line broadening experienced by these two peaks results from exchange to and from the unstructured state, the state which gives rise to the detectable resonace.

Since there were only minor changes in ^{15}N and ^{1}H chemical shifts for the amide protons between HSQC spectra collected at 1 M urea increments, it was possible to track with confidence the identities of many peaks (approximately 50%) assigned in the absence of urea through the series of spectra. To assign the new peaks and the peaks which could not be tracked with certainty, an HNCACB spectrum was obtained on Δ131Δ in 6 M urea. From the interresidue C_α and C_β correlations from this experiment plus the assignments that could be carried over from 0 M urea, 125 out of the 131 residues could be assigned. Figure 6 shows the sequential connectivities for the stretch of residue between S3 and V23.

With these assignments in 6 M urea, each "new" amide proton peak could be tracked through the $^{15}N-^{1}H$ spectra obtained at successively lower urea concentrations to determine the concentration at which it first appeared and how its intensity changed as a function of urea. In Figure 7, plots of peak intensity as a function of urea are shown, with the peaks grouped into two classes based on the urea concentration at which they first appear. One class of peaks disappears between 6 and 5 M urea and includes only residues between V23 and V39, whereas the second class disappears between 5 and 3 M urea and includes only residues between T13 and T22. In fact, all assigned residues in the segment between V23 and V39 disappear by 5 M urea, and all assigned residues between T13 and T22 are gone by 3 M urea. These

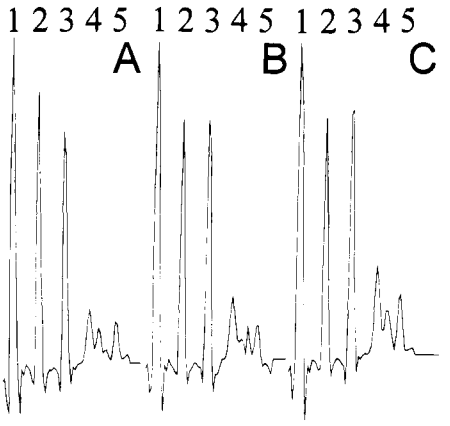

FIGURE 5: Relative peak intensity from three $^{15}N-^{1}H$ correlation spectra of Δ131Δ in 3.5 M urea obtained with different pulse sequences but constant $^{1}H \rightarrow ^{15}N \rightarrow ^{1}H$ magnetization transfer times (18 ms total). Panel A, conventional HSQC (Mori et al., 1995) with $^{1}/_{4}J_{NH}$ of 2.25 ms, plus a 2 × 2.25 ms ^{1}H spin echo delay in each direction. Panel B, HSQC with double-refocused INEPT, $^{1}/_{4}J_{NH}$ of 2.25 ms, plus a 2 × 2.25 ms ^{15}N refocusing relay in each direction. Panel C, cross-polarization 2D experiment with 9 ms Hartman−Hahn mixing time in each direction. This pulse sequence suppresses all line broadening during the magnetization transfer that arises from chemical exchange between conformations with different chemical shifts. Peak assignments: 1, I139; 2, G55; 3, A112; 4, K16; 5, A17. The latter two peaks are from residues in the β1 segment.

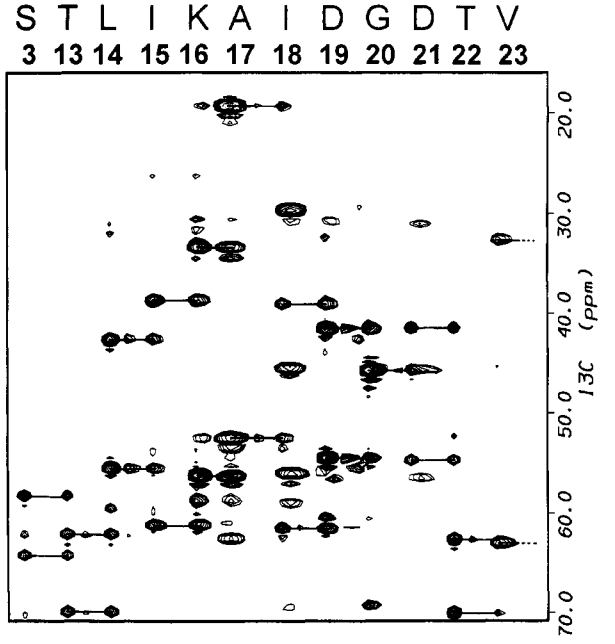

FIGURE 6: A composite spectrum of peaks from the HNCACB spectrum of Δ131Δ in 6 M urea demonstrating the sequential connectivities of C_α and C_β resonances for the 12 residues from S3 to V23 (residues 4−12 are not present in Δ131Δ).

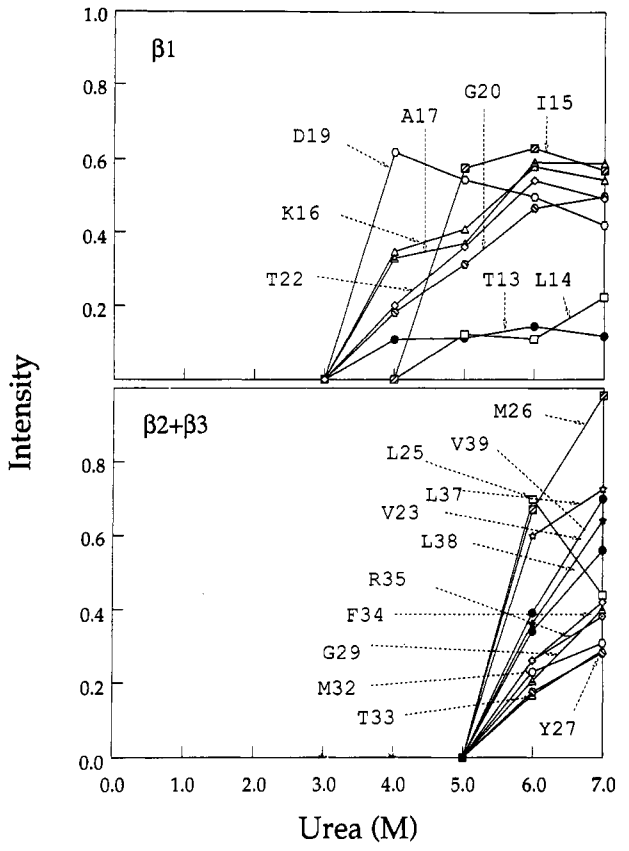

FIGURE 7: Graphs of the relative H_N peak intensities (normalized to the intensity of the carboxyl terminus, W140) as a function of urea concentration. Top panel, all assigned and tracked peaks from residues in the β1 segment (T13 to T22). Bottom panel, all assigned and tracked peaks from the β2-β3 segment (V23 to F34) plus L37, L38, and V39.

data are consistent with two sequential reactions as the urea concentration is lowered, one involving structure formation of residues in β2 and β3 and the other involving β1. The simplest explanation is that β2 and β3 form a two-strand β hairpin, followed by addition of β1 to generate a native-like three-strand antiparallel β sheet, a "β meander".

In addition to establishing connectivities, the HNCACB experiment gives the ^{13}C shifts of C_α and C_β, which have been shown to contain reliable information on secondary structure (Spera & Bax, 1991; Wishart et al., 1991). Figure 8 shows the secondary shifts of these resonances of Δ131Δ in 6 M urea and the differences in secondary shifts between 0 and 6 M urea. For reasons that are not clear to us, essentially all of the C_β resonances are shifted upfield in 6 M urea by approximately 0.5 ppm relative to their random coil values. Since the secondary shifts of the C_β are small in 0 M urea, the only structural conclusion that can be drawn from the C_β data is that, in 0 M urea, these resonances do not reveal any clear evidence of residual secondary structure.

Some of the variation in secondary shifts in C_α may be a consequence of local amino acid sequence effects (e.g., T41, K116, H121). Therefore, the difference in secondary shifts between 0 and 6 M urea may be the most reliable indicator of urea-sensitive residual structure. From the secondary shifts and changes in secondary shifts of the C_α resonances shown in Figure 8, the following patterns can be discerned: (1) a reduction in the helical population of α2 (residues 98−106) from 30% in 0 M urea to 10%−15% in 6 M urea, (2) a reduction in helical population of α1 (residues 57−68) from 10%−20% to below the level of detectability in 6 M urea, and (3) an indication that a small residual helicity in the third turn of helix α3 (residues 129−132) present in 0 M urea is eliminated in 6 M urea.

WT Nuclease at pH 3.0. To characterize the residual structure in staphylcoccal nuclease denatured by an entirely different perturbation, studies were undertaken of full-length wild-type nuclease at low pH. The midpoint of acid denaturation is approximately pH 3.7, and the effective number of protons taken up on denaturation is between 5 and 6 (Anfinsen et al., 1972). Therefore, at pH 3.0, wild type nuclease is more than 99% denatured. Since previous studies in this pH range have indicated that high salt concentrations can lead to significant aggregation (Meeker and D. Shortle, unpublished observations), the ionic strength was minimized by extensively dialysis of purified nuclease against distilled/deionized water. At pH 3.0, nuclease has a net charge of approximately +20, so the Cl^- concentration is probably at least 30−40 mM at the protein concentrations used for NMR spectroscopy.

Figure 9A shows the far-ultraviolet CD spectrum of nuclease at pH 3.0 in 20 mM glycine-hydrochloride buffer. The very weak ellipticity between 210 and 230 nm suggests that the acid-denatured state has less persistent secondary structure than does Δ131Δ in the absence of urea. As high concentrations of urea are added, this small amount of structure is reduced. As shown in Figure 9B, the difference spectra between 0 M urea and 2, 4, and 6 M urea also have the single minimum around 215 nm characteristics of β sheet structure. However, the depth of the minimum in the 0−6 M difference spectrum is only half as large as that obtained with Δ131Δ at pH 5.3, indicating that WT nuclease at pH 3.0 lacks some of the β sheet content present in the Δ131Δ fragment model of the denatured state.

The $^{15}N-^{1}H$ correlation spectrum of WT, pH 3.0, is shown in Figure 10. A total of 132 peaks can be resolved. This form of nuclease contains 18 more amino acids than Δ131Δ, 14 of which reside in a floppy amino-terminal extension (residues 1−6) and a carboxy-terminal extension (residues 142−149). Since fewer than 100 backbone amide protons are resolved for Δ131Δ in the absence of urea, this number of peaks suggests that some of the amide protons not seen in Δ131Δ may be present in the spectrum of WT, pH 3.0.

To obtain sequential assignments of WT, pH 3.0, the three-dimensional NMR experiments HNCACB, {$^{1}H-^{15}N$}-TOCSY-HSQC, and {$^{1}H-^{15}N$}-NOESY-HSQC were carried out. From these data, 117 out of 132 peaks could be assigned plus four of the five prolines. These include essentially all assigned residues in Δ131Δ in 0 M urea plus several residues between T13 and T22. However, just as in the case of Δ131Δ, no peaks corresponding to residues between V23 and E43 were found. From these three experiments, the chemical shifts of H_α, C_α, and C_β were obtained, and the secondary shifts for these resonances are plotted as a function of sequence in Figure 11. In addition, NOEs involving assigned amide protons are also shown schematically. These data suggest that most of the structural elements identified in Δ131Δ in 0 M urea are also present in this quite different denatured state.

From the magnitude of the C_α and H_α chemical shifts plus NOEs involving the H_N, the following statements can be made about the persistent structure in WT, pH 3.0: (1) α2 is approximately 30% populated, (2) α1 and α3 are less than

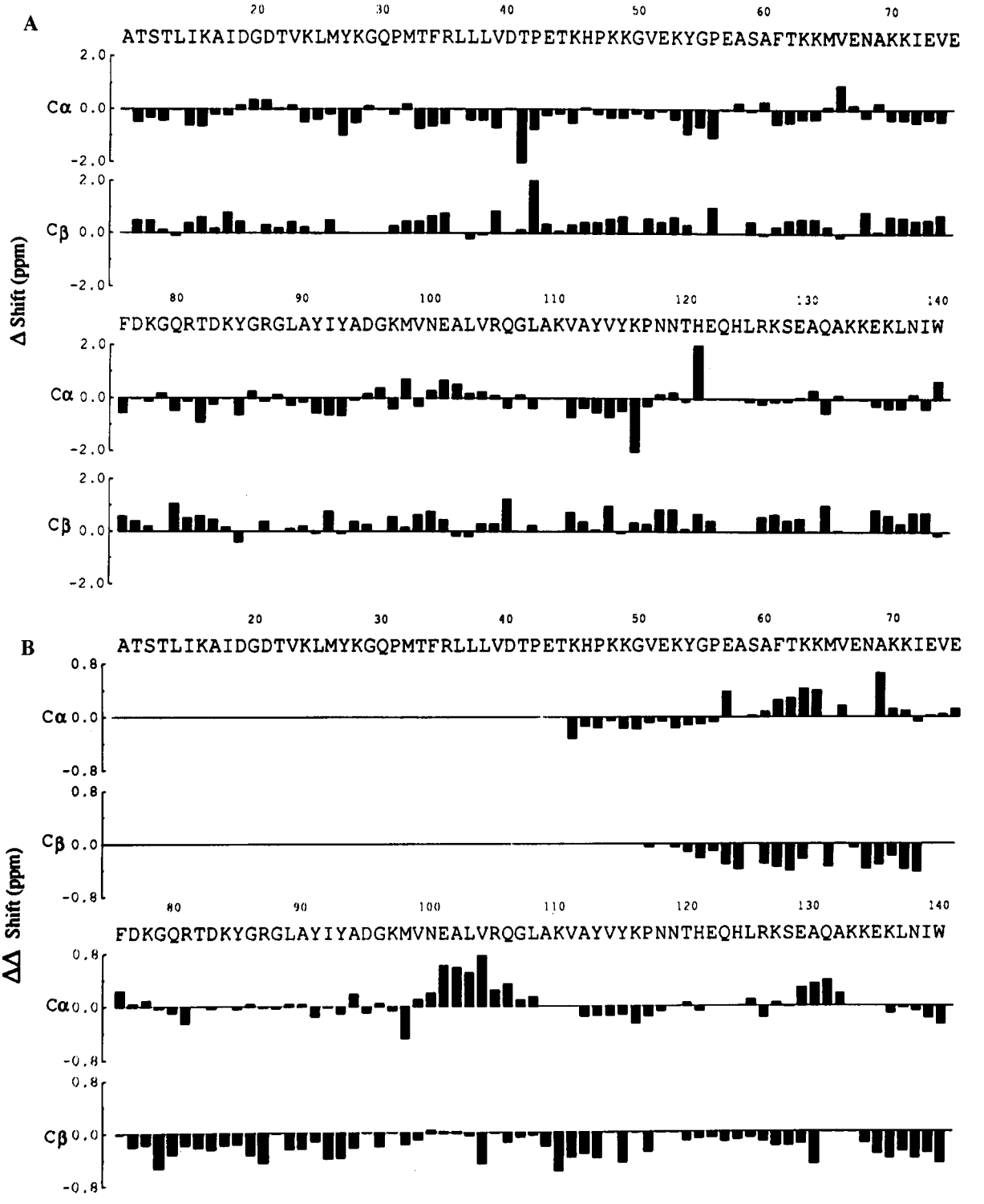

FIGURE 8: (A) Histograms of the secondary shifts (Δshift = observed chemical shift − random coil chemical shift) of the $^{13}C_\alpha$ and $^{13}C_\beta$ resonances of Δ131Δ in 6 M urea. The random coil values of Spera and Bax (1991) were used. (B) Histograms of the changes in the secondary shifts of the $^{13}C_\alpha$ and $^{13}C_\beta$ resonances of Δ131Δ between 0 and 6 M urea (ΔΔshift = Δshift in 0 M urea − Δshift in 6 M urea).

10% populated, (3) the type I′ turn involving residues 94−97 appears highly populated, (4) the type I turn formed by residues 83−87 is populated, but significantly less so than in Δ131Δ, (5) no clear evidence of β structure is seen for β4 and β5, and (6) the β meander involving β1-β2-β3 is inferred to be significantly populated from the severe line broadening of all of these residues except those around the tight turn between β1 and β2.

CONCLUSIONS

The β hairpin formed by strands β2-β3 appears to be the most stable secondary structural element in staphylococcal nuclease. At concentrations of urea below 6 M, all of the H_N for residues between V23 and V39 disappear in concert, and upfield shifting of the ^{13}C carbonyl resonances plus minimum at 215 nm in the circular dichroism spectrum are both suggestive of increasing β sheet structure. The only

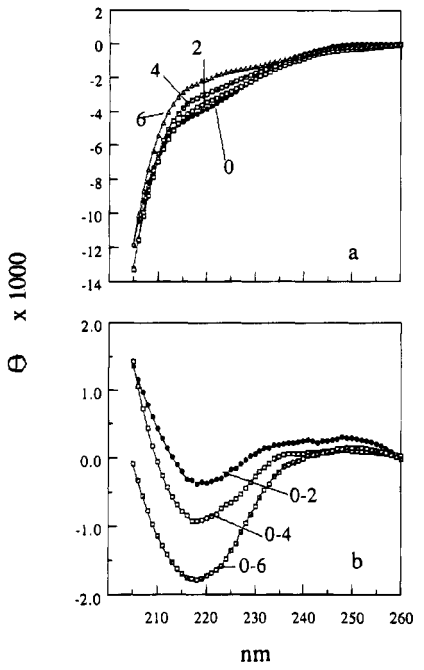

FIGURE 9: (A) Far-ultraviolet circular dichroism spectra of WT nuclease at pH 3.0, 32 °C, as a function of urea concentration, 0−6 M. The *y*-axis is the ellipticity in deg cm^2 dmol^{-1}. (B) Difference spectra obtained by subtracting the 2, 4, and 6 M spectra from the 0 M urea spectrum, to approximate the spectra of the structure lost upon addition of urea.

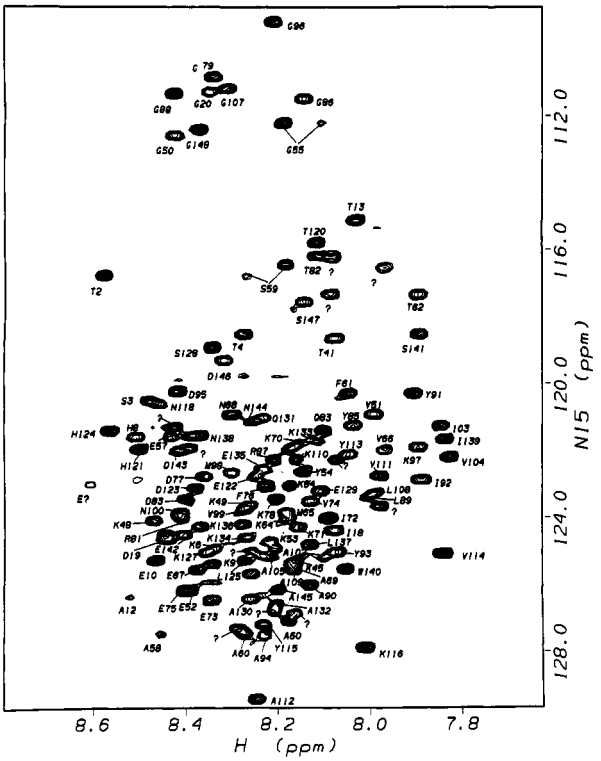

FIGURE 10: ^{15}N−^{1}H correlation spectrum (HSQC) of WT nuclease at pH 3.0, 32 °C, with peak assignments.

plausible mechanism for the severe fine broadening affecting the H_N, ^{13}C, and other resonances of a contiguous stretch of residues is conformational exchange on a slow to intermediate time scale between multiple conformations with different chemical shifts.

Four lines of evidence suggest that this broadening is caused by exchange between multiple structured conformations, not exchange between a structured and an unstructured state. (1) The 1D ^{13}C carbonyl spectra revealed only broad, upfield-shifted peaks for residues in the β1-β2-β3 segment. Peaks with the chemical shifts expected for the random coil-like state were not observed until high urea concentrations. (2) No set of $^{1}H_N$ peaks with chemical shifts suggestive of a structured state has been sent under any conditions (Alexandrescu et al., 1994; Wang et al., 1995). (3) All H_N peaks disappear at approximately the same rate as the urea concentration is lowered. If broadening resulted from exchange between the random and the structured state, the extent of broadening would depend on the difference in the ^{1}H and ^{15}N chemical shifts between the states, a value that is likely to vary significantly among the different residues. (4) Only a small amount of conformational exchange broadening of peaks corresponding to the unstructured state of β strand β1 in 3.5 M urea could be demonstrated by measuring the relative increase in peak intensity when cross polarization (which suppresses all chemical shift differences for both ^{1}H and ^{15}N during magnetization transfer) is used as opposed to the conventional HSQC (which does not suppress chemical shift differences during these fixed delays). Therefore, the intensities of the observed H_N peaks for residues in the β1-β2-β3 segment at a given concentration of urea probably reflect the fractional population of the unstructured state at that concentration.

The observation that the β2-β3 β hairpin is stable under such severe conditions can be explained by the fact that a large amount of nonpolar surface area is buried on formation of this structure. An analysis by Moult and Unger (1991) of the hydrophobic surface buried per residue upon going from a hypothetical fully extended state to the native secondary structure identified residues V23 to F34 as burying 60.3 Å^2/residue, more than any other segment of length 12 in staphylococcal nuclease. In fact for all of the 19 proteins in their study, only four segments of length 12 buried a greater amount of hydrophobic surface. It is noteworthy that the third-ranked segment of nuclease in this study consists of residues M98 to A109, which buries 50.3 Å^2/residue upon formation of α helix α2. This hydrophobic helix also is relatively stable, being populated to a level of approximately 30% in buffer and persisting to an estimated 10%−15% in 6 M urea.

In native nuclease, β strand β3 ends at residue R35 (Loll & Lattman, 1989), and the adjacent hydrophobic segment L36-L37-L38-V39 forms long-range contacts with β5, α3, and other chain segments. The observation that residues L37(38), L38(37), and V39 disappear below 6 M urea raises the possibility that these residues interact with the β2-β3 hairpin, perhaps by binding to its hydrophobic face. This model is very strongly supported by recent studies of Δ131Δ variants containing either the mutations, L37G or V39G. In both cases, *all* of the β1-β2-β3 H_N resonances are observable in 0 M urea and are quite sharp by 2 M urea (Y. Wang and D. Shortle, unpublished observations). Such a local, non-native interaction (Figure 12) could stabilize the hairpin and also protect it from unfavorable interactions with other hydrophobic surfaces, either in the same or different polypeptide chains. To complete the folding of nuclease, the hairpin must dock with β-strands β4 and β5 to form the native β barrel. Presumably the energetic cost of breaking down such a local, non-native interaction in a later folding step is small, this hydrophobic segment only having to move to one side

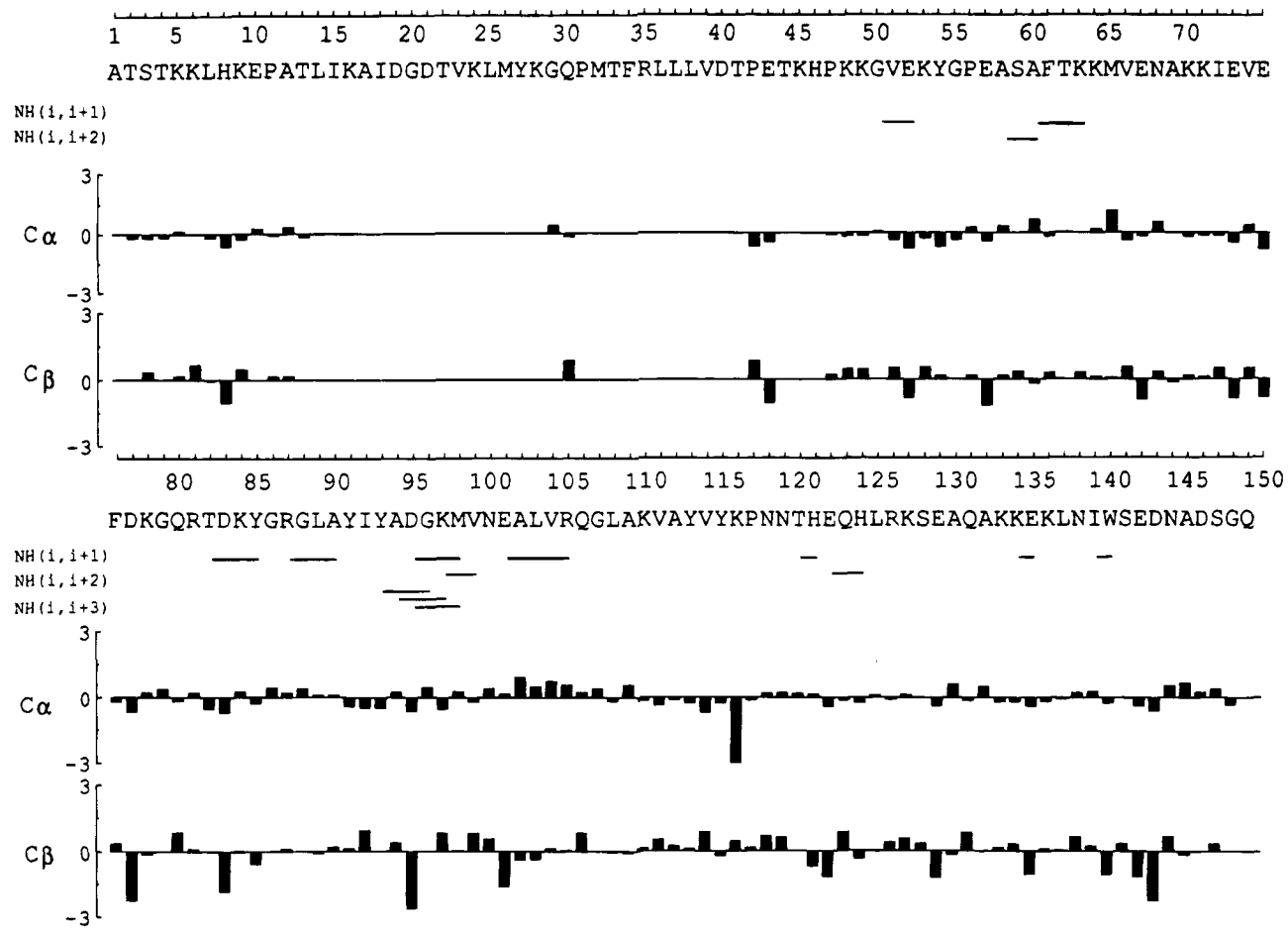

FIGURE 11: Diagram of the H_N-H_N NOEs and the secondary shifts of the $^{13}C_\alpha$ and $^{13}C_\beta$ resonances of WT nuclease at pH 3.0. The random coil values of Spera and Bax (1991) were used. No $H_\alpha-H_N$ NOEs between i and $i + 2$, 3, or 4 could be unequivocally assigned.

in order to form its final contacts in the native state.

A detailed study of the backbone dynamics of Δ131Δ by ^{15}N relaxation suggested that a segment extending from the tight turn at 83−87 through strand β5 and helix α2 is relatively rigid, with an effective rotational correlation time of approximately 8 ns (Alexandrescu & Shortle, 1994). Preliminary analysis of the three dimensional relationships of the secondary structural elements in Δ131Δ by paramagnetic relaxation from nitroxide spin labels linked to unique cysteine mutant sites provides direct evidence for a close interaction between α2 and β4-β5 (J. Gillespie and D. Shortle, unpublished data), an interaction not seen in the native state. As with β2-β3 hairpin, it appears that a local, non-native interaction driven by hydrophobic forces may serve to stabilize native-like segments of supersecondary structure. It is reasonable to propose this may be a common mechanism of protein folding: elements of native supersecondary structure are stabilized by local non-native interactions which can be easily undone and restructured into a native format upon merger with other supersecondary structural elements. Algorithms for identifying such metastable supersecondary structures would contribute significantly to the prediction of protein tertiary structure.

Prior to formation of the five-strand β barrel, β strand β1 appears to add on to the β2-β3 hairpin, forming a three-strand antiparallel β meander. The evidence for this is the relatively concerted disappearance of all of the H_N for the segment between T13 and T22 between 5 and 3 M urea, the continued increase in a β strand component in the CD spectrum, and the upfield shifting of the ^{13}C carbonyl resonances for I15 and I18 below 4 M urea.

Although only minimal changes are seen in the resonances from chain segments β4 and β5 as a function of urea concentration, previous work has shown that addition of glycerol leads to the rapid broadening of residues in the β4-β5 segment plus the continued increase in the beta strand component of the CD spectrum (Wang et al., 1995). Control experiments on WT native nuclease suggested that most of this broadening is not a consequence of the increase in solution viscosity, which is known to directly decrease proton T_2's by increasing the rotational correlation time. For the same reasons cited above, these data in glycerol are more consistent with severe broadening resulting from exchange between multiple structured conformations than exchange between a structured state and a nonstructured or random state.

Δ131Δ is denatured because several residues have been removed from the amino and carboxy termini of wild-type nuclease. To determine how representative the residual structure found in Δ131Δ is, a preliminary structural analysis is also reported here of WT full-length nuclease denatured by low pH and low salt concentrations. Comparison of their CD spectra and $^1H-^{15}N$ correlation spectra suggest these two denatured states have a great deal in common. Secondary chemical shifts for C_α, C_β, and H_α plus intensities of NOEs involving amide protons reveal only three significant differences. First, the CD spectrum suggests WT, pH 3.0, has less residual β strand character, which is consistent with the

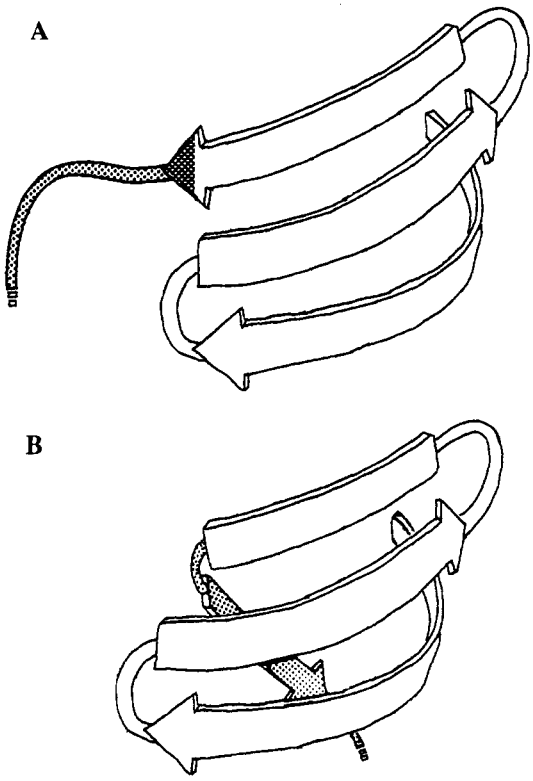

FIGURE 12: Ribbon diagram of the native and a hypothetical non-native structure formed by the segment of nuclease between T13 and V39, which includes the β1-β2-β3 segment plus four large hydrophobic amino acids, L36, L37, L38, and V39, which are shown in grey.

NMR evidence for partial disruption of the residues in and near the tight turn between strands β1 and β2. This finding suggests that protonation of carboxyl residues, presumably D19 and/or D21, is partially disrupting the interaction between β1 and β2-β3. Secondly, on the basis of several medium-range H_N-H_N NOEs, the type I turn involving residues 83−87 appears to be less populated than in Δ131Δ. Again, the presumption can be made that protonation of a carboxyl group in or near this chain segment (possibly D83) is destabilizing the tight turn. And finally, the negligible helical structure detected in helix α1 may be a consequence of protonation of one of the glutamates (E57 or E67) in this chain segment.

From this comparison of two very different denatured states, it apears that the fractional population of α2, the significant population of type I′ turn between residues 94 and 97, and the formation of a dynamic structure involving the β meander β1-β2-β3 are constant features of the residual structure in denatured nuclease in the absence of strong denaturants. Important for future studies of denatured nuclease is the finding that the chemical shifts of the amide proton of a specific residue is, if detectable, more or less unchanged by alterations in solution conditions. Only small changes in $^{15}N-^{1}H$ coordinates were seen for the H_N in Δ131Δ as the urea concentration was varied from 0 to 7 M urea. Similarly, relatively small differences were found for most residues between the H_N coordinates of Δ131Δ at pH 5.3 in 0 M urea and WT nuclease at pH 3.0. Although peak assignments cannot be carried over from one denatured state to another with confidence, this rough constancy of ^{1}H and ^{15}N chemical shifts does permit tentative assignment of a new spectrum. Such provisional assignments, plus the finding that disappearance of peaks is correlated with the formation of an ensemble of interconverting structures, allow some of the structural differences between different denatured states to be inferred. A preliminary survey of the $^{1}H-^{15}N$ correlation spectra of severely destabilizing mutants of nuclease, many of which are single-residue insertions (Sondek & Shortle, 1990, 1992), suggests that different subsets of structure are being affected by different mutations (Y. Wang and D. Shortle, unpublished data).

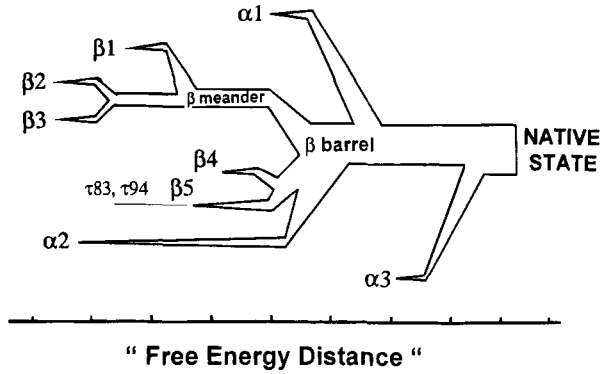

FIGURE 13: Schematic diagram of the equilibrium folding pathway of nuclease based on data presented in this report plus data from Wang et al. (1995). Except for the helix α1, the *y*-axis corresponds to the amino acid sequence from amino terminus (top) to carboxy terminus (bottom).

From the results in this report plus earlier data on the structural changes in Δ131Δ accompanying increases in glycerol concentration (Wang et al., 1995), a very tentative hierarchical equilibrium folding pathway can be proposed. As shown schematically in Figure 13, this pathway can be drawn as a series of clustering events along an axis equivalent to a "free energy distance". Upon lowering the urea concentration from 6 to 0 M, the β2-β3 hairpin forms first, followed by the addition of β1 to form the β1-β2-β3 meander. In addition, the population of the hydrophobic α helix α2 increases from 10−15% to approximately 30%. By 0 M urea, the two tight turns involving residues 83−86 and 94−97 that flank strand β5 are highly populated and helix α1 becomes partially populated. As the glycerol concentration is increased from 0% to 30%, a rapid increase in β structure seen by CD and NMR suggests that β4 and β5 are merging with the β1-β2-β3 meander to form the five-strand β barrel, which represents the hydrophobic core of nuclease (Shortle et al., 1990). At still higher concentrations of glycerol, CD and NMR spectroscopy suggest that helices α1 and α2 may fully form, with the very last step being the formation and docking of helix α3 to complete the native structure.

It has been brought to our attention by a colleague that the most stable structural elements (i.e., β1-β2-β3) are at the amino terminus and the least stable (α3) is at the carboxy terminus, a pattern that may have some relevance to the folding of nuclease in vivo, either in the cell or after transport into the extracellular space.

ACKNOWLEDGMENT

We thank Julie Forman-Kay for pointing out the merits of direct detection of the ^{13}C carbonyl resonances, Chitrananda Abeygunawardana for help with several of the NMR experiments, Lewis Kay for the pulse sequences for the HNCACB, HNCO, TOCSY-HSQC, and NOESY-HSQC

experiments, and Joel Gillespie for help with the CD spectroscopy.

REFERENCES

Abragam, A. (1961) *The Principles of Nuclear Magnetism*, Oxford University Press, London.
Alexandrescu, A. T., & Shortle, D. (1994) *J. Mol. Biol. 242*, 527–546.
Aexandrescu, A. T., Abeygunawardana, C., & Shortle, D. (1994) *Biochemistry 33*, 1063–1072.
Anfinsen, C. B., Schecter, A. N., & Taniuchi, H. (1972) *Cold Spring Harbor Symp. Quant. Biol. 36*, 249–255.
Dill, K. A., & Shortle, D. (1991) *Annu. Rev. Biochem. 60*, 795–825.
Dobson, C. M. (1992) *Curr. Opin. Struct. Biol. 2*, 6–12.
Jardetzky, O., & Roberts, G. C. K. (1981) *NMR in Molecular Biology*, Academic Press, New York.
Johnson, W. C., Jr. (1988) *Annu. Rev. Biophys. Biophys. Chem. 17*, 145–166.
Kuwajima, K. (1989) *Proteins: Struct. Funct. Genet. 6*, 87–103.
Logan, T. M., Theriault, Y., & Fesik, S. W. (1994) *J. Mol. Biol. 236*, 637–648.
Loll, P. J., & Lattman, E. E. (1989) *Proteins: Struct. Funct. Genet. 5*, 183–201.
Matthews, C. R. (1993) *Annu. Rev. Biochem. 62*, 653–683.
Mori, S., Abeygunawardana, C., Johnson, M. O., & van Zijl, P. C. M. (1995) *J. Magn. Reson. B 108*, 94–98.
Morris, G. A., & Freeman, R. (1979) *J. Am. Chem. Soc. 101*, 760.
Moult, J., & Unger, R. (1991) *Biochemistry 30*, 3816–3824.
Muhandiram, D. R., & Kay, L. E. (1994) *J. Magn. Reson. B 103*, 203–216.
Neri, D., Billeter, M., Wider, G., & Wuthrich, K. (1992) *Science 257*, 1559–1563.
Shortle, D. (1993) *Curr. Opin. Struct. Biol. 3*, 66–74.
Shortle, D., & Abeygunawardana, C. (1993) *Struture (London) 1*, 121–134.
Shortle, D., Stites, W. E., & Meeker, A. K. (1990) *Biochemistry 29*, 8033–8041.
Sondek, J. E., & Shortle, D. (1990) *Proteins: Struct. Funct. Genet. 7*, 299–305.
Sondek, J. E., & Shortle, D. (1992) *Proteins: Struct. Funct. Genet. 13*, 132–140.
Spera, S., & Bax, A. (1991) *J. Am. Chem. Soc. 113*, 5490–5491.
Tiffany, M. L., & Krimm, S. (1973) *Biopolymers 12*, 575–587.
Wang, Y., Alexandrescu, A. T., & Shortle, D. (1995) *Phil. Trans. R. Soc. London, Ser. B 348*, 27–34.
Wishart, D. S., Sykes, B. D., & Richards, F. M. (1991) *J. Mol. Biol. 222*, 311–333.
Woody, R. W. (1992) *Adv. Biophys. Chem. 2*, 37–79.
Yamazaki, T., Pascal, S. M., Singer, A. U., Forman-Kay, J. D., & Kay, L. E. (1995) *J. Am. Chem. Soc. 117*, 3556–3564.

BI951751U